Contents lists available at SciVerse ScienceDirect

Chemical Engineering Research and Design

journal homepage: www.elsevier.com/locate/cherd

A comparative activity study of a new ultra-dispersed catalyst system for a hydrocracking/hydrotreating technology using vacuum residue oil: Merey/Mesa

Gladys Noguera[a], *Solange Araujo*[b,*], *Javier Hernández*[a], *Angel Rivas*[a], *Dietrich Mendoza*[b], *Olga Castellano*[a]

[a] *PDVSA-Intevep, Gerencia General de Refinación e Industrialización, a Gerencia de Investigación Estratégica, Apartado 76343, Caracas 1070-A, Venezuela*

[b] *Gerencia de Refinación, Apartado 76343, Caracas 1070-A, Venezuela*

A B S T R A C T

Ultra-dispersed catalysts give an improvement over the main reactions activity by having a low deactivation rate. They provide as well other advantages like a diminution in the catalysts metal concentration, a reduction in contaminants and also these catalysts can be used in almost every area where heterogeneous catalysts are used. Catalysts synthesis optimization is important to improve process recovery, especially in hydrocracking/hydrotreating processes, where feedstock is vacuum residue. Here, we have evaluated the catalytic performance of two molybdenum–nickel catalysts prepared using different emulsion formulation, named E-T (base catalyst) and AT-48 (new catalyst). Our results showed that, the percentage of converted products for VR 500 °C$^+$, asphaltenes and microcarbon are comparable for both E-T and AT-48 catalysts, despite the fact that for the latter a lower molybdenum concentration was used. In addition, post-catalytic particles analyses using SEM and TEM techniques demonstrated that AT-48 catalyst showed a non-aggregated and homogeneous narrower distribution of metallic particles than E-T one. The lower average particle size distribution is related to the improvement of the liquid product yields for the hydroconversion of Mery/Mesa VR using the AT-48 catalyst.

Keywords: Ultra-dispersed catalyst; AHM; Hydrocracking; Hydrotreating; Hydroprocessing

1. Introduction

The use of ultra-dispersed catalysts becomes an ideal alternative to treat heavy feedstocks and petroleum residues because high dispersion of metallic species is obtained. Therefore, an elevated activity toward main reactions of interest (Panariti et al., 2000a,b; Marchionna et al., 1994), are reached because of a high ratio area/volume. It is known that heterogeneous catalysts also have a high activity, but in addition they have a high deactivation rate which reduces their use in processes that work with high quantities of contaminants.

Ultra-dispersed catalysts can be classified as: heterogeneous and homogeneous depending on their miscibility under reaction conditions. Homogeneous catalysts can be divided in soluble compounds in aqueous phase or in organic phase. Heterogeneous solids are introduced to the process through dry dispersion of the catalytic solid or precursor, finely divided into the crude (Ren et al., 2004; Thompson et al., 2008). Main disadvantage of heterogeneous solids is that they have a lower activity and generate by products of difficult handling.

In addition, soluble metallic precursors are highly reactive, but they have an elevated cost to be use at high scale. In the other hand, soluble compounds in aqueous phase are injected to process as catalytic emulsions, with the advantage that these precursors are cheaper in comparison with the organometallics.

Currently, new technologies aim to use ultra-dispersed catalysts, prepared from metallic precursors soluble in aqueous phase (Intevep, 2000). PDVSA Intevep has been developing technologies in order to obtain deep conversion for

* *Corresponding author*. Tel.: +58 212 3306129; fax: +58 212 3307230.
E-mail addresses: nogueragS@pdvsa.com, araujosc@pdvsa.com (S. Araujo).
Received 7 September 2011; Received in revised form 22 March 2012; Accepted 16 April 2012
0263-8762/$ – see front matter © 2012 The Institution of Chemical Engineers. Published by Elsevier B.V. All rights reserved.
http://dx.doi.org/10.1016/j.cherd.2012.04.006

Nomenclature

A	absorbance
b	path length of the cell (cm)
BC	base concentration (ppm)
C_x	concentration of anion x (M)
$X_{500\,^\circ C^+}$	vacuum residue 500 °C$^+$ conversion (wt%)
$X_{asphaltenes}$	asphaltene conversion (wt%)
ε_x	absorption coefficient of anion x ($M^{-1}\,cm^{-1}$)

valorization of heavy and extra-heavy crude oils of the Orinoco Oil Belt (OOB). At this point in time, our technological developments have been successfully tested in catalytic transformation of different type of VR from OBB, reaching up to 95 wt% of VR 500 °C$^+$ conversion with a high yield to light distillated products and low rejection to coke. These catalytic formulations are based on emulsions w/o, prepared by an aqueous phase dispersion of molybdenum and nickel in heavy vacuum gasoil (HVGO), containing a surfactant. Molybdenum aqueous phase Mo(VI), is an ammonium thiomolybdates solution, prepared *in situ* by sulfurization of a metal dissolution with a sulfiding agent. This sulfurization of Mo(VI) dissolution involves a series of consecutive reactions described in Eqs. (1) and (2) (Harmer and Sykes, 1980). Thiomolybdates solution is emulsified and injected at process, where the active catalytic specie is generated *in situ* by thermal decomposition (Eq. (3)):

$$Mo_7O_{24}^{6-} + 4H_2O \Leftrightarrow 7MoO_4^{2-} + 8H^+ \quad (1)$$

$$MoO_4^{2-} + 4H_2S \Leftrightarrow MoO_{x-4}S_4^{2-} + H_2O \quad (2)$$

$$(NH_4)_2MoS_4 + H_2 \xrightarrow{\Delta} MoS_2 + 2H_2 + 2NH_3 \quad (3)$$

In this work, a study relating to the effect of the catalytic precursors sulfurization grade on hydroconversion activity, of two molybdenum–nickel dispersed catalyst formulations, for the vacuum residue 500 °C$^+$ Merey/Mesa, is presented. In order to evaluate catalytic formulations performance, changes in the operation conditions, regarding concentration of hydrogen sulfur in the reactor and additive particle size, were taking into account.

2. Experimental

This section shows a feedstock, catalysts, additives and products characterization; and also, a description of the experimental procedure.

2.1. Feedstock

The vacuum residue 500 °C$^+$ Merey/Mesa, was used as feedstock for the deep conversion process. This residue is a mixture of 53% (v/v) Merey crude and 47% (v/v) Mesa crude. The vacuum residue Merey/Mesa was characterized in accordance with standard procedures and properties are listed in Table 1.

2.2. Catalysts

The catalytic systems evaluated in this study, consist of two ultra-dispersed catalyst from w/o emulsions of Mo/Ni differentiated by the Mo metal concentration and pre-sulfide treatment. In both cases, the active specie in these formulations are generated *in situ* through thermal decomposition of the emulsified system in a high pressure reduction environment.

Table 1 – Properties of feedstock VR Merey/Mesa.

Parameter	Merey/Mesa
Gravity API at 60 °C	5
Carbon (wt%)	84.3
Hydrogen (wt%)	11.05
Total sulfur (wt%)	3.28
Nitrogen (wt%)	0.76
V (ppm)	432
Ni (ppm)	104
Asphaltenes (n-C_7 insolubles) (wt%)	18.71
Asphaltenes (IP-143) (wt%)	19.3
Toluene insolubles (wt%)	0.122
Microcarbon (wt%)	21.7
TAN (mg KOH/g)	0.65
Kinematic viscosity at 100 °C (cSt)	18,936
Kinematic viscosity at 135 °C (cSt)	1299
Ashes (wt%)	0.019
Saturates (wt%)	13
Aromatics (wt%)	41
Resins (wt%)	31
Asphaltenes (wt%)	15
Residue 500 °C$^+$ (wt%)	96.3

Table 2 – Properties of HVGO Merey/Mesa.

Parameter	Merey/Mesa
Gravity API at 60 °C	17.9
Carbon (wt%)	85.29
Hydrogen (wt%)	12.74
Total sulfur (wt%)	2.02
Nitrogen (wt%)	1826
V (ppm)	0.001
Ni (ppm)	<1
Asphaltenes (n-C_7 insolubles) (wt%)	0.1
Asphaltenes (IP-143) (wt%)	<0.5
Toluene insolubles (wt%)	0.02
Microcarbon (wt%)	0.26
TAN (mg KOH/g)	1.33
Kinematic viscosity at 100 °C (cSt)	11.94
Kinematic viscosity at 135 °C (cSt)	4.317
Ashes (wt%)	0.0037
Saturates (wt%)	50
Aromatics (wt%)	46
Resins (wt%)	4
Asphaltenes (wt%)	<1

Catalyst preparation had several stages. First stage consisted in preparing a solution of Mo(VI), by direct dissolution of ammonium heptamolybdate (AHM) in a sulfiding agent, at a determined composition and temperature with constant stirring. Two aqueous solutions were obtained, with differences between the metal concentration and sulfurization pretreatment.

The second stage consisted of dispersing each aqueous solution with a HVGO-surfactant mixture. The HVGO properties are showed in Table 2. This mixture was homogenized with mechanical stirring.

Two catalysts were synthesized. The first one was prepared starting with a Mo solution partially presulfurated in solution. This formulation is completely sulfurated after being emulsified. Second catalytic emulsion was prepared starting with a Mo solution, completely sulfurated, in where MoS_4^{2-} was maximized, without solids precipitation. The first emulsion

Fig. 1 – E-T drop size distribution.

was called E-T, while the sulfurated in solution was called AT-48. Drop size distribution of catalytic molybdenum emulsions, E-T and AT-48, are shown in Figs. 1 and 2, respectively.

Due the catalyst is formed by a Mo/Ni mixture, a nickel emulsion was prepared similarly to molybdenum emulsion (E-T). The nickel acetate tetrahydrated salt was dissolved in this solution (with a specific concentration) and incorporated in the organic matrix, which had been previously contacted with the surfactant. Both emulsion Mo and Ni are injected separated to the process avoiding precipitation of Ni. The active specie Mo/Ni is created *in situ* by thermal decomposition of the emulsions.

2.3. Additives

The conversion process applied in this study, uses an organic additive with the main finality of minimizing the formation of foam in the reactor, controlling temperature, adsorbing contaminants (asphaltenes and metals) and possibly serving as a support for the active catalytic species for some of the chemical reactions that take place in the reaction zone. In this test, the additive was first sieved to adjust the average size of the particles; two average sizes (X_{50}) were used: 19.9 μm (Fig. 3) and 94.8 μm (Fig. 4).

Fig. 2 – AT-48 drop size distribution.

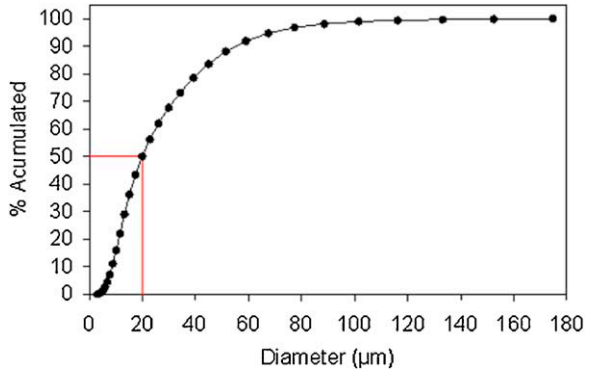

Fig. 3 – Particle distribution, X_{50} = 19.9 μm.

2.4. Pilot plant

The catalysts performance was tested using a pilot plant with one reactor with a total volume of 1200 ml. This reactor has five heating zones, in where five isothermic furnaces are placed. The pilot plant has an additive injection system, a feedstock and gas preheating systems, emulsion tanks, recycle and feed, a high pressure high temperature separator, a three-phase separator, heavy and light product tanks, and a sampling system. The process flow diagram of this unit is shown in Fig. 5.

2.4.1. Pilot plant test procedure

Test procedures for evaluating the catalyst performance, using both formulations (E-T and AT-48), were the same. Details of the procedure are as follows (see Fig. 5).

VR is pumped continuously from the feedstock tank to the preheater. This VR is previously mixed with the additive (<3 wt%), DMDS/Gasoil mixture (which acts as sulfiding agent), emulsions and the preheated recycle gas (350–370 °C). Emulsions injection is done sequentially, first molybdenum emulsion is injected and then nickel emulsion. Average molybdenum experimental concentration respect to feedstock for E-T will be referred as base concentration (BC), concentration for AT-48 will be from 60% to 65% of BC, and nickel concentration is given by the ratio:

$$\frac{[Ni]}{[Ni]+[Mo]} \cong 0.2 \text{ when working with BC (refers to E-T)} \quad (4)$$

$$\frac{[Ni]}{[Ni]+[Mo]} \cong 0.3 \text{ when working with 65\% of BC (refers to AT-48)} \quad (5)$$

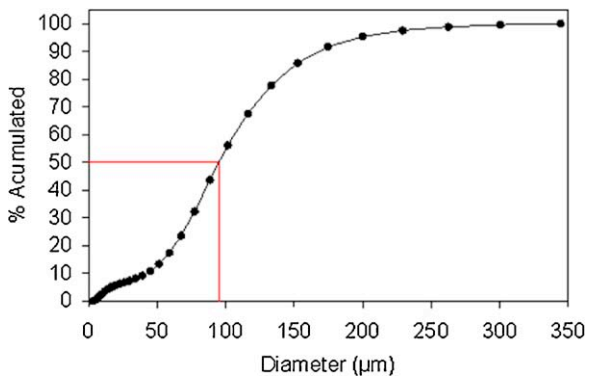

Fig. 4 – Particle distribution, X_{50} = 94.8 μm.

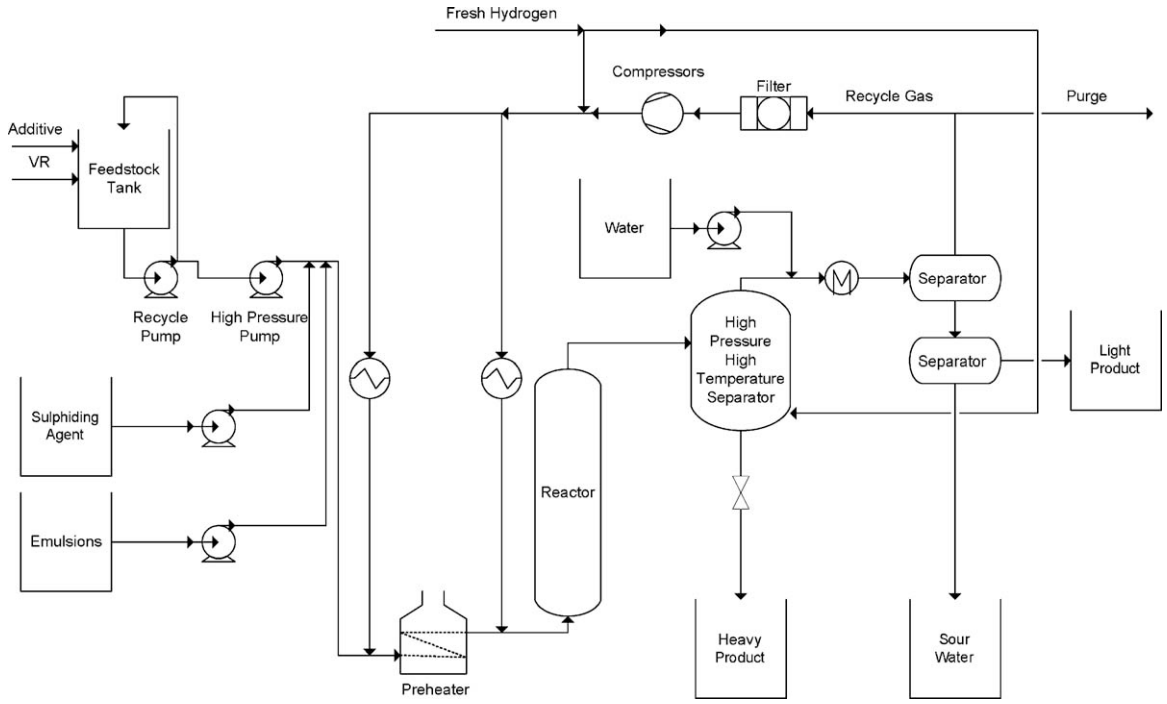

Fig. 5 – Process flow diagram of the pilot plant.

At the preheater, mixture is heated until reaching a maximum temperature of 445 °C. In this preheater, molybdenum emulsion is dehydrated, decomposed and sulfurizated, generating the active phase, MoS_2, which is the reaction active center inside of the reactor.

After the preheater, mixture is injected to the reactor. This reactor has five heating zones monitored by thermocouples, distributed equally in each zone, inside (thermowell in the center of the reactor) and outside of the reactor (reactor wall). This reactor is a bubble column reactor, which not uses any internals to do phase distribution. Fluids in this reactor enter at the bottom and flow cocurrent upwards. Temperature is controlled by the difference in temperature measurements between thermocouples inside and outside the reactor at the same level.

Reactor product flows toward the high pressure high temperature separator (330 °C and 2160 psig), where is separated in two streams, top and bottom. At the top there are light products, H_2S and NH_3. This stream, also called hot separator top (HST), is washed with H_2O and then is sent to an exchanger, in where light products are condensed. This stream, that also contains gases and water, goes to a separation stage, where the gas, sour water, and light products are separated and sent to purge/recycle, light product tank and sour water tank, respectively.

Bottom product from the high pressure high temperature separator goes to the let-down valves, to reduce pressure, and then to the heavy product tank, this product is also called hot separator bottom (HSB). This stream contains unconverted residue, organic additive, metals and coke that could be produced in the reaction zone.

In Table 3 operation conditions for each part of the test are given.

Should be noticed that for conditions 1 and 2 recycle gas was used and for conditions 3 and 4 only fresh hydrogen was used.

2.4.2. *Characterization*

Light and heavy products were analyzed to compare catalysts performance. Samples were taken following the same procedure each time and especial care was taken for the bottom product in order to obtain a homogenized sample. In this case, constant nitrogen bubbling at the bottom of the heavy product tank was maintained, in all stages of process. For carrying out sampling, the first container was always discharged, to avoid a high solid content in the sample due to sedimentation and accumulation in the bottom of the tank. Light products were taken, carefully, in glass jars that were sealed after sampling to avoid lighters leak from the jar.

It should be noticed that it is beyond the scope of this article analysis related to gas products, and for that matter results taking into account gases are not shown in the following sections.

The catalysts and feedstock were sampled during the whole test to ensure the stability of the emulsions, the metal

Table 3 – Operation conditions.

#	Catalyst	[Mo]	$\frac{[Ni]}{[Ni]+[Mo]}$	T (°C)	P (psig)	LHSV (h^{-1})	Particle size (μm)
1	E-T	BC	0.2	445	2159	0.4	19.9
2	AT-48	65% BC	0.3	445	2159	0.4	19.9
3	AT-48	60% BC	0.3	445	2160	0.4	19.9
4	AT-48	60% BC	0.3	445	2159	0.4	94.8

and water concentration inside of the tanks and the organic additive concentration.

All samples were taken every 24 h after mass balance, was closed. Results were taken as acceptable if the mass balance had a ratio percentage of $mass_{out}/mass_{in}$, around $100 \pm 2\%$.

From each sample, a global product distribution was determined.

2.4.2.1. Catalysts characterization. In this section it would be explained the catalyst characterization.

2.4.2.1.1. Quantification of the concentration of species $Mo_xS_{4-x}^{2-}$ formed in solution. Thiomolybdate-forming reactions in solutions were monitored by UV–vis absorption spectroscopy. However, the extensive overlap in the spectra has hindered data from the UV–vis characterization. As a consequence, in order to make the accurate quantification of the composition of thiomolybdate mixtures, sample characterization data was analyzed using the linear function. The spectra were recorded on a PerkinElmer model Lambda 35 Spectrophotometer, using 1 cm quartz cuvette and deionized water as the blank solution.

Concentrations of individual thiomolybdate anions were calculated based on the principle that total absorbances of a mixture at any wavelength is equal to the sum of the absorbance of the components at that wavelength. Beer's Law equations and the four thiomolybdate anions were calculated by fitting these equations using multiple linear regressions and the experimental data obtained; molar absorptivity coefficients were taken from literature (Erickson and Helz, 2000). The thiomolybdate anions concentration obtained for AT-48 was 50 wt% higher that E-T.

2.4.2.1.2. Particle size of UD catalyst and additives determination. Drop size distribution of catalytic emulsions was determined by optical microscopy, with a microscope Olympus BX51 (see Figs. 1 and 2). The organic additive particle distribution, as dust, was determined using static laser scattering particle size distribution analyzer Horiba (Partica LA-950 V2). Measurement range is between 0.1 and 3000 μm. Solid was dispensed using a vibrator feeding device (see Figs. 3 and 4).

2.4.2.1.3. Compositional analysis. The emulsion metallic content (Mo and Ni), was measured by fluorescence spectroscopy X-ray, using a Panalytical device, model Axions Petro. The samples were taken at the beginning and during the pilot plant test in the stored tanks, after each mass balance was closed.

2.4.2.2. Feedstock characterization. The feedstock characterization was monitored by toluene insolubles during the test, to assure that a constant concentration of the organic additive was pumped to the reaction zone. This measure was considered for all conversion calculations.

2.4.2.3. Light and heavy products characterization. Light products were characterized using two laboratory test: API gravity and simulated distillation (ASTM D-2887). The characterization of the heavy product was carried out using six laboratory tests: API gravity, toluene insolubles, asphaltenes IP-143, heptane (n-C_7) insolubles, microcarbon (ASTM D-4530) and simulated distillation using standard procedures (ASTM D-7169 and ASTM D-1160). Heavy product analyses allowed calculating VR 500 °C$^+$, asphaltenes and microcarbon conversion percentage. The percentage conversion of VR 500 °C$^+$ is given by

$$X_{VR500\,^\circ C^+} = \frac{VR_{Inlet} - VR_{HSB} - \text{Net coke}}{VR_{Inlet}} \times 100 \quad (6)$$

It should be noticed that asphaltenes conversion was calculated using toluene insolubles and IP-143, taking into account that the last is considered more accurate, but the first one is faster and can be used to follow pilot plant response in a short period of time.

2.4.2.4. Post-catalytic particles characterization. The post-catalytic particles were separated from the heavy product and characterized as follows.

Post-reaction catalysts were obtained from HSB, which contains unconverted residue, HVGO, metallic particles, organic additive and rejected carbon from reactor. The recovery process was carried out by extraction of HVGO and residue from HSB, using soxhlet extractions with CH_2Cl_2 as solvent. The insolubles solids containing coke and metallic particles were rigorously subjected to a scrutiny by electron microscopy. The morphology and elemental composition were determined using scanning electron microscopy (SEM) and the size using transmission electron microscopy (TEM). The SEM and TEM analyses were carried out using a high performance Jeol JSM6480 LV with, and a Jeol JEM 2100, with an acceleration voltage of 200 kV, respectively.

Finally, Mo and Ni metal content was determined using an ICP-OES Horiba Jobin Yvon Active.

3. Results and discussion

Pilot plant had a total of 1036 h in stream. Thirty six mass balances closed in the acceptable range (10 for condition 1, 13 for condition 2, 5 for condition 3 and 8 for condition 4) with an average ratio percentage of $mass_{out}/mass_{in}$, around $99 \pm 1\%$. In this section reactor inspection, conversions, liquid product yields and post-catalytic studies, are presented, according to the 36 mass balance products.

3.1. Reactor inspection

After 1036 h in stream in pilot plant almost no fouling was found inside of the reactor, as shown in Fig. 6(a). It could be seen that the solid inside of the reactor was easily removed (Fig. 6(b)) and it represented part of the organic additive mixed with the feedstock. This behavior is typical of good hydrogenation catalysts, meaning that VR 500 °C$^+$ and asphaltenes are converted with a low rejection to carbon or low coke yield during the test, which is a very desirable property for a hydrocraking/hydrotreating catalyst. However, it is also true that pilot plant for hydroprocess was operated at moderate high pressure/temperature condition and an increase of rejection to petcoke could be probably expected from severe operation conditions. Nevertheless, E-T emulsion formulation has been proven on not only at high severe conditions but also in a bigger scale pilot plant, with a similar performance of the catalyst relating to coke yields.

3.2. Conversions

VR 500 °C$^+$ conversions values presented in Fig. 7 were calculated using only data from ASTM D-7169 method, due to

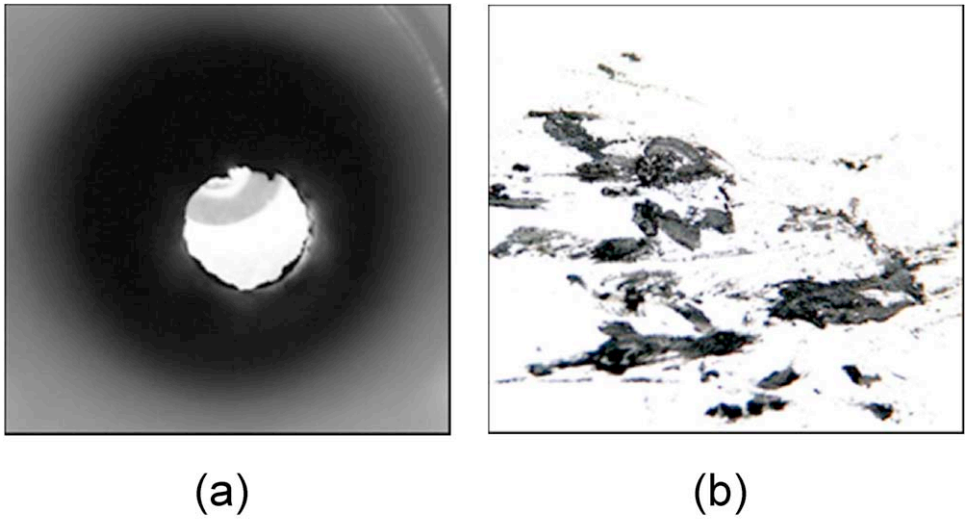

Fig. 6 – Reactor inspection after shutdown.

statistical results obtain for ASTM D-7169 and ASTM D-1160, using Miller and Freund (1977) and Rorabacher (1991) methods, presented no difference between their averages. Using the same statistical tests, also, it could be concluded that VR 500 °C$^+$ conversion values remained constant during the whole test, and it was equal to 66.9 ± 2.6 wt%, showing no particular effect over conversion values when the formulations were changed. It should be noticed a low value conversion was reached because operating conditions were worked at moderate severity as was mentioned above. The results showed that, under conditions tested in here, both catalysts, AT-48 and E-T, had a similar performance, when VR Merey/Mesa was tested. It is important to mention that AT-48 has up to 40 wt% less molybdenum concentration than the typical E-T catalyst, which represents an advantage because of the molybdenum costliness.

Asphaltenes conversions are presented in Fig. 8, these conversions were calculated using IP-143 method, which has a better accuracy than heptane (n-C_7) insolubles method. For conditions 1 and 2, asphaltenic fraction showed a similar conversion behavior than VR 500 °C$^+$, where no change was observed when catalyst emulsion formulation was replaced under the same operational condition of the pilot plant. Calculated average percentage was 68.0 ± 2.4 wt% for conditions 1 and 2. On the other hand, the average conversions values of asphaltenes for condition 3 and 4 were 64.5 ± 1.4 wt% and 58.0 ± 3.3 wt%, respectively. These results show a decreasing of 4% and 10% in the conversion percentage values with respect to conditions 1 and 2, but also a difference in the conversion between condition 3 and 4.

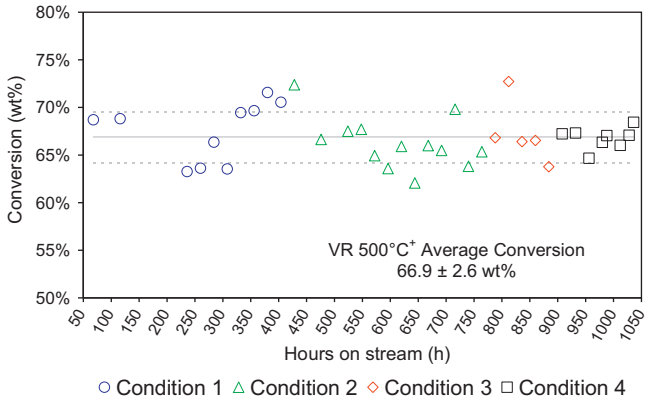

Fig. 7 – VR 500 °C$^+$ conversions.

The different conversion behavior observed in this study was attributed to the changes in the operating condition of the pilot plant. Under conditions 3 and 4 gas recycle was turned off and the pilot plant was operated under fresh constant hydrogen flow, while in condition 4 the organic additive was replaced with an additive having particles with a larger average size distribution (≈100 μm). As consequence, hydroprocessing performance for asphaltenes conversion under conditions 3 and 4 was affected.

The reasons why only the asphaltenes conversion decreased when the H_2S/H_2 ratio decreased are not so clear so far. A first cause could be related to an incomplete catalyst sulfurization under reaction environment and the second could be attributed to the direct participation of H_2S in the transformation reactions of this kind of molecules. In both cases, a decreasing in the hydrogenation efficiency could be expect either by a lower concentration of sulfiding species catalytically active and because the more difficult asphaltenes hydrogenation reactions cannot take place in a low H_2S concentration environment.

By the other hand, the poor asphaltenes conversion performance under condition 4 was probably due to changes in the reactor fluid dynamic or a trapping effect over asphaltenes when an organic additive with larger particles was used. In this sense, Fukuyama and Terai (2007) have reported that active carbon due to its mesopore structure it is able to selectively adsorb asphaltenes. Further investigations are being carried out to study the observed effects and improving hydroconversion of asphaltenic fractions.

Finally, microcarbon conversions are shown in Fig. 9, and not significant differences were obtained in the hydroconversion percentages during the whole test. Microcarbon conversion showed a similar behavior as VR 500 °C$^+$ conversion, where percentages of conversion were kept nearly constant in the four tested conditions. This result indicates

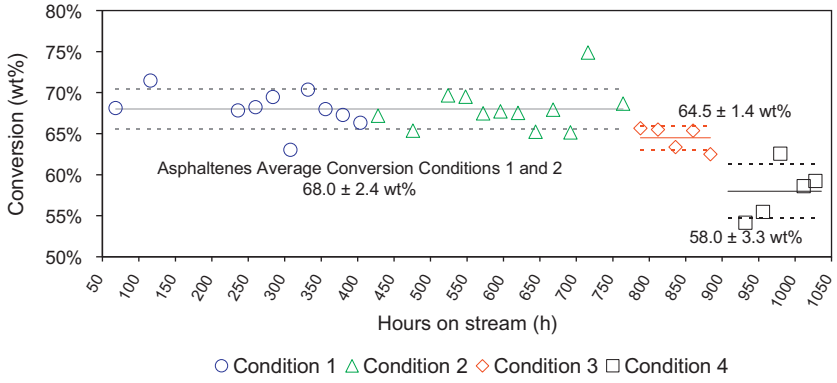

Fig. 8 – Asphaltenes conversions.

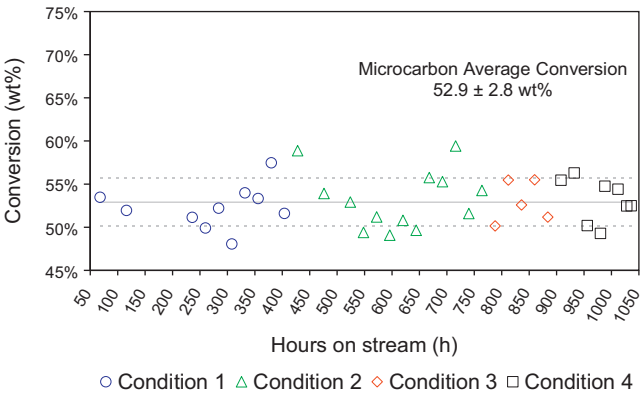

Fig. 9 – Microcarbon conversions.

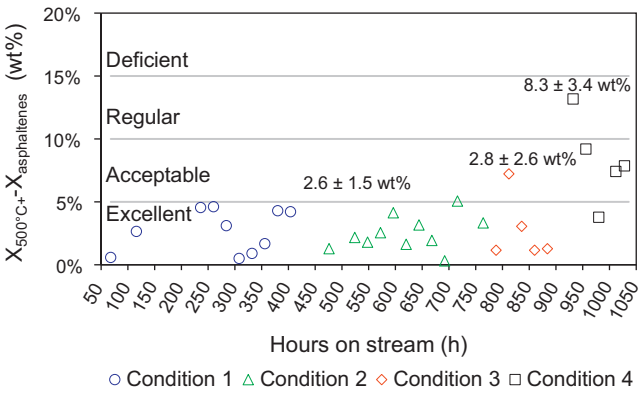

Fig. 10 – Hydrogenation respect to asphaltenes conversion.

that rejection reactions to carbon products or petcoke were not affected by changes in the operation conditions of pilot plant. Catalytic formulation change or particle size variation of organic additive does not diminish microcarbon conversion but also does not affect adversely this value.

3.3. *Hydrogenation*

The hydrogenation efficient is a well-known parameter used to establish a measuring of the performance of catalytic processes. This parameter relates the fraction of converted asphaltenes and the fraction of converted feedstock 500 °C⁺. For ratios close to the unit a good hydrogenation function is reached. In Table 4, the average $X_{asphaltenes}/X_{500\,°C^+}$ ratios calculated from the percentage values of asphaltenes and RV 500 °C⁺ conversions are presented for each operational condition. It can be observed that a good hydrogenation function for all conditions was obtained. As expected from the low asphaltenes conversion, condition 4 has a lower $X_{asphaltenes}/X_{500\,°C^+}$ ratio than the others pilot plant operation conditions.

Also, another criteria for hydrogenation efficiency that consists in the difference between $X_{500\,°C^+}$ and $X_{asphaltenes}$ was taken into account. When a difference of less than 5 wt% is

Table 4 – Ratio $X_{asphaltenes}/X_{500\,°C^+}$.

Condition	$X_{asphaltenes}/X_{500\,°C^+}$
1	1.0
2	1.0
3	1.0
4	0.9

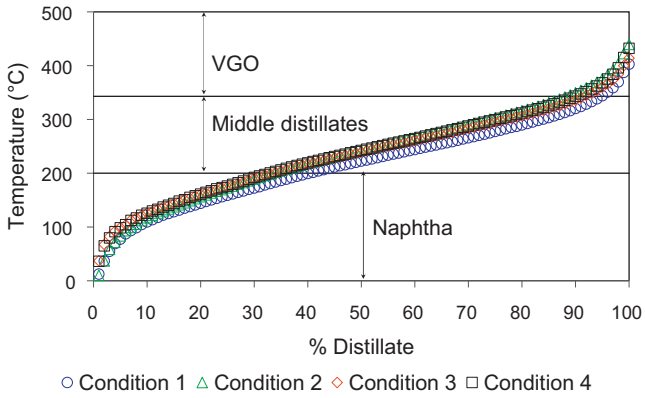

Fig. 11 – HST product distribution.

obtained an excellent hydrogenation is reached (see Fig. 10). For conditions 1–3, hydrogenation efficiency was excellent while for condition 4, hydrogenation was only acceptable. These findings are in concordance with results in Table 4.

3.4. *Liquid product yields*

For both tested formulations, E-T and AT-48, not significant difference could be observed between distributions of HST and HSB products (Figs. 11 and 12). This is a desirable result since formulation AT-48 has around 40% less molybdenum concentration than E-T formulation, which represents a reduction in terms of costliness of the process catalyst. In fact, a slightly improvement around 2–3 wt% on the overall conversion of RV 500 °C⁺ was achieved when AT-48 formulation was used. In addition, the quality of liquid products showed a similar percent behavior in the yield's distributions (see Fig. 13). The AT-48

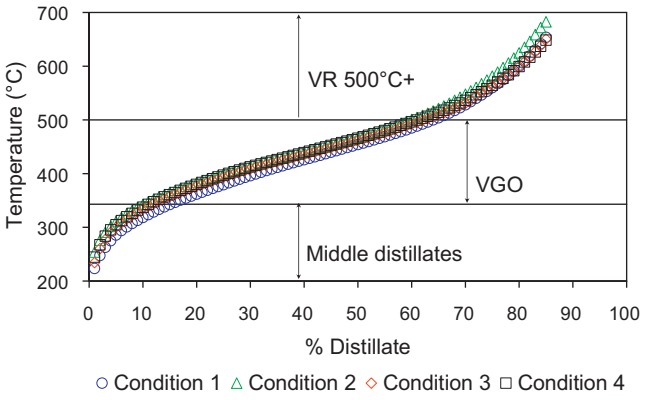

Fig. 12 – HSB product distribution.

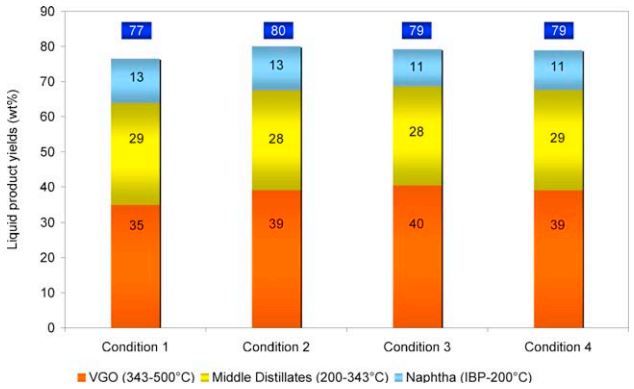

Fig. 13 – Syncrude yields.

catalyst gives a more valuable syncrude product, depicted the fact a 2 wt% decrease of naphta yield is observed when AT-48 catalyst is used under pilot plant operational conditions 3 and 4 without gas recycle. Once again, partial H_2S pressure seems to play an important role in the hydrogenation of the different products. The decrease of the naphta yield could be also related to the decrease of asphaltenes conversion, if it is assume that a fraction of the naphta products have their source in the hydrocracking/hydrogenation reactions of the asphaltenic fraction. The effects of the H_2S partial pressure over the catalytic activity of metallic sulfides has been reported elsewhere (Panariti et al., 2000b). In HDS and HYD reactions, both promotion and inhibition effects of the catalytic activity has been observed as consequence of H_2S concentration (Farag et al., 2009). Catalytic performance as a function of metal, presence of other metallic promoters and the metallic particle sizes, among others, has been related to the partial pressure of H_2S Nadège et al., 2004.

3.5. *Post-catalysts particles*

The E-T and AT-48 post-reaction solids were isolated from HSB product obtained under test conditions 1 and 2, by using CH_2Cl_2 as extraction solvent. As was expected, isolated solids showed a high amount of carbon content (≥94%) from coke products. However, SEM and TEM techniques were useful to detect nanometallic particles attributable to catalyst under carbonaceous matrix. Table 5 displays the chemical composition of the samples, for the selected surface area depicted in Fig. 16, as was determined using SEM-EDS technique. Some appreciable differences can be observed from compositional results of E-T and AT-48 solid samples. Both samples show a similar low metallic content of Mo and Ni metals, but Ni percentage was slightly higher in sample AT-48 than E-T.

Table 5 – Chemical composition by SEM-EDS.

Elements	E-T Atomic (%)	AT-48 Atomic (%)
C	95.12	94.19
O	1.94	3.08
S	1.91	1.78
V	0.48	0.53
Ni	0.20	0.26
Mo	0.16	0.16

Only slightly differences were found for sulfur and vanadium contents. The latter was considering to be recovered by the demetallation of feedstock; since this metal was not present in any reagent used. Also, traces of Fe and Cl were observed on the SEM-EDS analyses.

The TEM micrograph images of particles of E-T and AT-48 samples and their corresponding size distributions histograms are shown in Figs. 14 and 15. In both images, nanosized particles with a size distribution range 2–10 nm and 1–6 nm were measured for E-T and AT-48 samples, respectively. Also, E-T sample micrograph shows some large aggregated particles with a size distribution range from 10 to 30 nm. It is interesting that AT-48 sample has the narrowest particle size distribution, depicted the fact a complete sulfurization was expected since the lower ratio Mo/S of this catalyst formulation.

These results indicated that the catalyst with the narrowest distribution size (AT-48) showed a similar or better performance that the base catalyst (E-T) having a lower Mo concentration. This finding has been reported in the literature by Panariti et al. (2000a) who studied the upgrading of heavy feedstocks in VR, using dispersed catalyst based on transition metal, and they found that catalyst with the lowest particle size has the highest catalytic activity and selectivity.

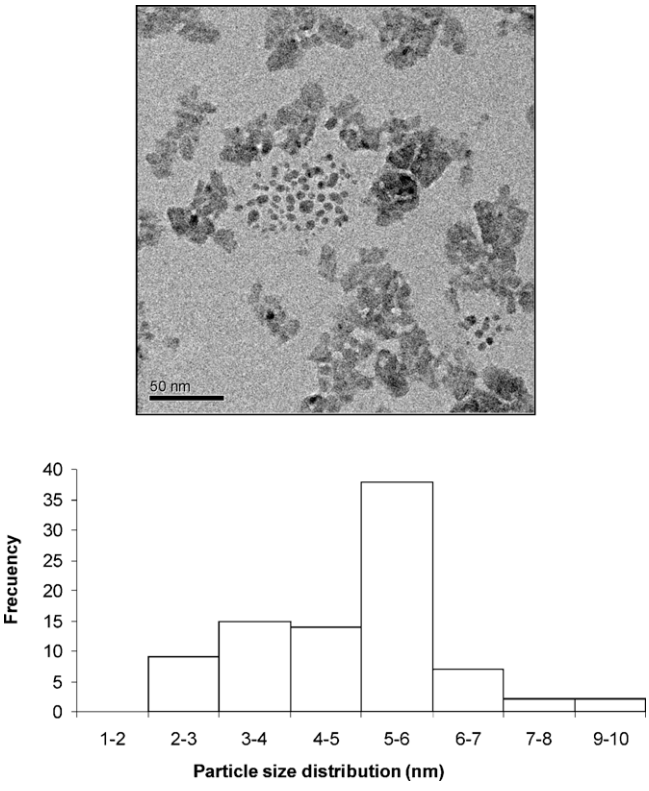

Fig. 14 – Micrograph and histogram of post-reaction E-T nano-particles distribution size.

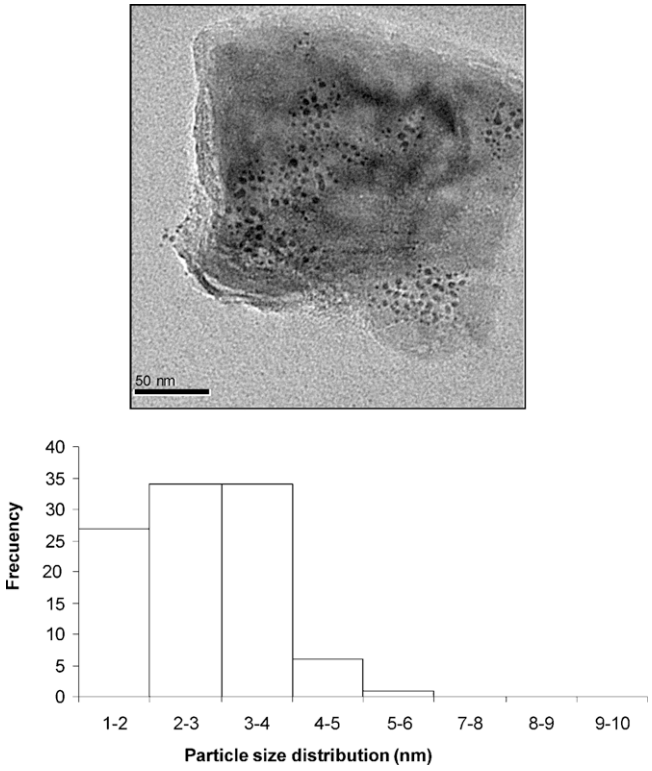

Fig. 15 – Micrograph and histogram of post-reaction AT-48 nano-particles AT-48 distribution size.

4. Conclusions

The importance of catalyst formulation has been demonstrated using two ultra-dispersed catalyst with different composition. The new catalyst AT-48 formulated using less molybdenum concentration showed a similar or better catalytic performance in the hydroconversion of Merey/Mesa VR than the base catalyst E-T.

The ultra-dispersed AT-48 and E-T catalysts reached the same $X_{500°C^+}$ (66.9 wt%), and almost the same liquid product yields (slightly higher when using AT-48), for middle distillates and naphtha (around 40%) and for residue (around 38%), for all conditions.

Asphaltene conversion was the same (68.0 wt%) for both formulations, when operating under the same conditions (recycle gas and particle size 19.9 μm), this conversion, had a decrease when recycle gas was change for fresh hydrogen, as a result on changes in the sulfur hydrogen partial pressure. Also a decrease in asphaltene conversion could be seen when particle size was increased until 94.8 μm. These results lead to the hypothesis that solid could act as a support to asphaltene reactions, which should be explore in further experiments.

For both catalysts a good hydrogenation could be reached, demonstrated with reactor inspection after shutdown, where no deposits could be found.

Post-reaction particles characterization by SEM revealed that the AT-48 formulation had a narrow distribution of metallic particles, with a lower average particle size, homogeneously distributed and without aggregated formation as observed in E-T formulation. This dissimilarity in size and dispersion of

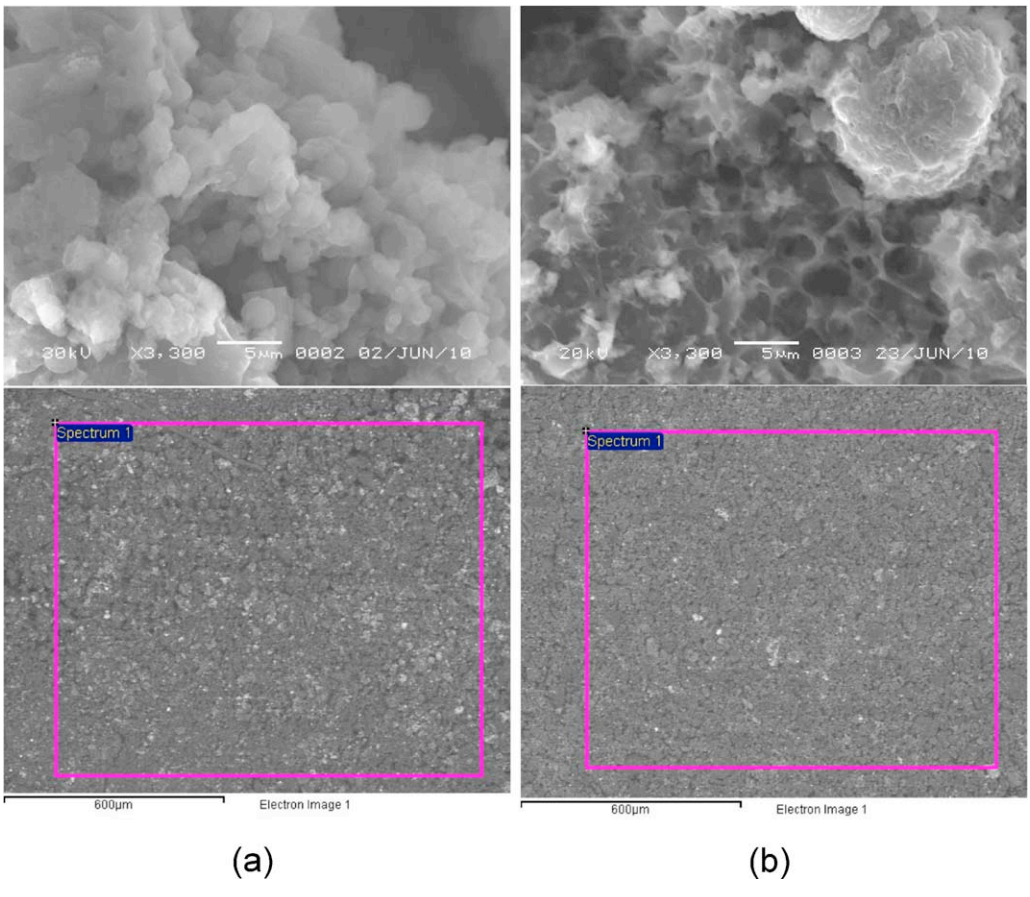

Fig. 16 – Post-reaction solids SEM images and zones for compositional analysis using EDS (a) E-T and (b) AT-48.

metallic particles for AT-48 and E-T, confirms that methodology used for emulsion sulfurization is actually affecting physic-chemical properties of catalytic active phases. Indeed the fact that AT-48 formulation showed a higher reactivity (since it had a lower concentration of molybdenum and reached the same results) toward the vacuum residue conversion could be related to a lower metallic particle size and a better metallic dispersion.

Acknowledgements

The authors thank to the personal operators of Pilot Plant Management at Intevep, S.A. by the valuable collaboration and excellent performance during whole test.

References

Erickson, B., Helz, G., 2000. Molybdenum(VI) speciation in sulfidic water: stability and lability of thiomolybdates. Geochim. Cosmochim. Acta 64, 1149–1158.

Farag, H., et al., 2009. Catalytic activity of synthesized nanosized molybdenum disulfide for the hydrodesulfurization of dibenzothiophene: effect of H_2S partial pressure. Appl. Catal. B: Environ. 91, 189–197.

Fukuyama, H., Terai, S., 2007. An active carbon catalyst prevents coke formation from asphaltenes during the hydrocracking of vaccum residue. Petrol. Sci. Technol. 25, 231–240.

Harmer, M., Sykes, G., 1980. Kinetics of the interconversion of sulfido- and oxomolybdate(VI) species $MoO_xS_{4-x}^{2-}$ in aqueous solutions. Inorg. Chem. 19, 2881–2885.

Intevep, S.A., 2000. Production of oil soluble catalytic. US Patent Number 6,043,182. Inventors: J. Cordova, P. Pereira, J. Guitian, A. Andriollo, A. Cirilo, F. Granadillo.

Marchionna, M., et al., 1994. Hydrotreating of petroleum residues with dispersed catalysts derived from thiomolybdates and molybdenyl acetylactonate. Fuel Process. Technol. 40, 1–14.

Miller, I., Freund, J., 1977. Probability and Statistics for Engineers, Second ed. Prentice-Hall Inc., USA.

Nadège, G., et al., 2004. Influence of H_2S on the hydrogenation activity of relevant transition metal sulfides. Catal. Today 98, 61–66.

Panariti, N., et al., 2000a. Petroleum residue upgrading with dispersed catalysts. Part 1. Catalysts activity and selectivity. Appl. Catal. A: Gen. 204, 203–213.

Panariti, N., et al., 2000b. Petroleum residue upgrading with dispersed catalysts. Part 2. Effect of operating conditions. Appl. Catal. A: Gen. 204, 215–222.

Ren, R., et al., 2004. Study on the sulfurization of molybdate catalysts for slurry-bed hydroprocessing of residuum. Fuel Process. Technol. 86, 169–178.

Rorabacher, D., 1991. Statistical treatment for rejection of deviant values: critical values of Dixon's "Q" parameter and related subrange ratios at the 95% confidence level. Anal. Chem. 63, 139–146.

Thompson, J., et al., 2008. The synthesis and evaluation of up-scalable molybdenum based ultra dispersed catalysts: effect of temperature on particle size. Catal. Lett. 123, 16–23.